J Comp Physiol A
DOI 10.1007/s00359-006-0130-9

ORIGINAL PAPER

On the barn owl's visual pre-attack behavior: I. Structure of head movements and motion patterns

Shay Ohayon · Robert F. van der Willigen · Hermann Wagner · Igor Katsman · Ehud Rivlin

Received: 28 September 2005 / Revised: 5 April 2006 / Accepted: 8 April 2006

Abstract Barn owls exhibit a rich repertoire of head movements before taking off for prey capture. These movements occur mainly at light levels that allow for the visual detection of prey. To investigate these movements and their functional relevance, we filmed the pre-attack behavior of barn owls. Off-line image analysis enabled reconstruction of all six degrees of freedom of head movements. Three categories of head movements were observed: fixations, head translations and head rotations. The observed rotations contained a translational component. Head rotations did not follow Listing's law, but could be well described by a second-order surface, which indicated that they are in close agreement with Donder's law. Head translations did not contain any significant rotational components. Translations were further segmented into straight-line and curved paths. Translations along an axis perpendicular to the line of sight were similar to peering movements observed in other animals. We suggest that these basic motion elements (fixations, head rotations, translations along a straight line, and translation along a curved trajectory) may be combined to form longer and more complex behavior. We speculate that these head movements mainly underlie estimation of distance during prey capture.

Keywords Motion parallax · Peering · Movement · Motor · Motor primitive

Abbreviation
3D Three-dimensional

Introduction

Many animals orient their gaze towards conspicuous objects, either by moving their eyes, heads, or both (e.g. Masino and Knudsen 1990; Haker et al. 2003). Owls are especially suited to investigate such orienting movements, because owls essentially lack eye movements (Steinbach and Money 1973; Du Lac and Knudsen 1990) so that changes in gaze may be directly derived from the analysis of head movements. The compensation for limited eye movements is manifested in a highly flexible neck that can rotate through very large angles (Masino and Knudsen 1990). Owls make conspicuous translational movements resembling peering movements that have been observed in other animals (Collett 1978; Sobel 1990; Kral and Poteser 1997; Troje and Frost 2000; van der Willigen et al. 2002; Kral 2003). While many naturalists and scientists have seen these movements, only one brief description has been published (Wagner 1989). We have initiated a systematic study of these head movements and their functional relevance. This manuscript deals with the structure of the head movements and with motion patterns. A

S. Ohayon · R. F. van der Willigen · H. Wagner
Institute of Biology II, RWTH University,
Kopernikusstrasse 16, 52074 Aachen, Germany

I. Katsman · E. Rivlin
Computer Science Department,
Israel Institute of Technology, Technion,
Haifa 32000, Israel

Present address: S. Ohayon (✉)
Computer Science Department,
Israel Institute of Technology, Technion,
Haifa 32000, Israel
e-mail: shayo@cs.technion.ac.il

subsequent report will concentrate on the functional relevance of the head movements (S. Ohayon et al., in preparation).

In general, head movements may contain both translational and rotational components. Previous studies in humans have compared head rotations to eye rotations and have suggested that both are governed by similar laws (Glenn and Vilis 1992; Medendorp et al. 1998). Two important laws for understanding human eye movements are Listing's law and Donder's law (Crawford et al. 2003). Donder's law states that the orientation of the eye when looking in a specific direction is always the same relative to the head coordinate system (Tweed et al. 1990). Listing's law states that rotation-vectors, describing eye orientations relative to the primary gaze direction, are confined to a plane known as Listing's plane (Howard 2002). Since eye movements in the barn owl are extremely limited, we set to investigate whether their head rotations are also governed by similar laws.

Measurements of eye, head or body movements in laboratory situations with restricted animals and natural settings with animals being able to move freely have a long tradition (e.g. Robinson 1963; Knudsen et al. 1979; Wagner 1982; Zeil 1993; van der Willigen et al. 2002). There has always been a tradeoff between precise, high spatial resolution that can be achieved in laboratory situations, but restricts the animal's movements, and recordings in natural settings that do not restrict the animal's movements, usually at the cost of spatial resolution. In order to describe the barn owls' head movements in this investigation, we took advantage of recent developments in camera and computer technology. This allowed us to recover both head position and orientation of unconstrained barn owls using a single camera (S. Ohayon and E. Rivlin, in preparation) and to apply techniques of differential geometry to analyze the data.

Previous stimulation experiments with barn owls have suggested six different categories of movements: saccadic head rotations, head translations, facial movements, vocalizations, limb movement and twitches (Masino and Knudsen 1993). Some of these categories may be regarded as high-level or complex description of movements. Action-related research, on the other hand, often starts from basic components of movements, termed, for example, motion primitives (Moeslund et al. 2005) or motion atoms (Campbell and Bobick 1995), and combines these to complex behavior (Bizzi et al. 1995; Mussa-Ivaldi and Bizzi 2000; Konczak 2005). The main thrust of this paper is to detect possible basic elements of motion and to give examples on how they may combine to longer, more complex behavior.

Materials and methods

Two male adult barn owls (*Tyto alba pratinocla*), SL and PT, were tamed by hand rearing and could be easily handled. No attempt was made to reverse the owls' nocturnal cycle. To maintain the owls' interest in food, their weight was maintained at approximately 85–90% of their ad-libitum weight. They received the necessary food, two dead chicks, in the course of the experiment. No positive reinforcement was given. The experimental procedures were approved by the Regierungspräsidium Köln.

Methods to measure head movements

Head movements may be represented using a rigid body transformation that takes into account all six degrees of freedom (three for translation and three for rotation). To describe how a rigid-body object, such as the owl's skull, rotates and translates in three dimensions (3D), one needs to define a coordinate system for it that moves relative to a fixed reference frame. In the following sections we will use the notation of $[X, Y, Z]$ to describe position or orientation of the owl's head in the camera coordinate system and [Pitch, Yaw, Roll] to describe position or orientation of movements in the owl coordinate system.

The movement of the rigid body may be represented by the transformation necessary to align the coordinate system of the object to that of the fixed reference frame. There are several ways to represent this transformation. The most common is the center of mass representation, which relates two points P and P' using the following rule: $P' = RP + T$ where P is an arbitrary point on the object, represented in the object coordinate system. P' corresponds to point P, but is represented in the fixed coordinate system. P is first rotated and then translated. R is a 3×3 rotation matrix, and T is a 3×1 translation vector. R represents the orientation of the object coordinate system in the fixed coordinate system and can be decomposed to three Euler angles, or to an angle and a rotation axis (both descriptions are equivalent). The latter is also known as rotation-vector representation. T represents the position of the object's center of mass in the fixed reference frame. This framework will be referred to as R–T representation. This representation describes translations well, but it is not well suited for the description of head rotation, since a translational component might also exist when rotation is not about the center of mass (Fig. 1).

Another way to describe a rigid body transformation is the helical axis representation (Medendorp et al.

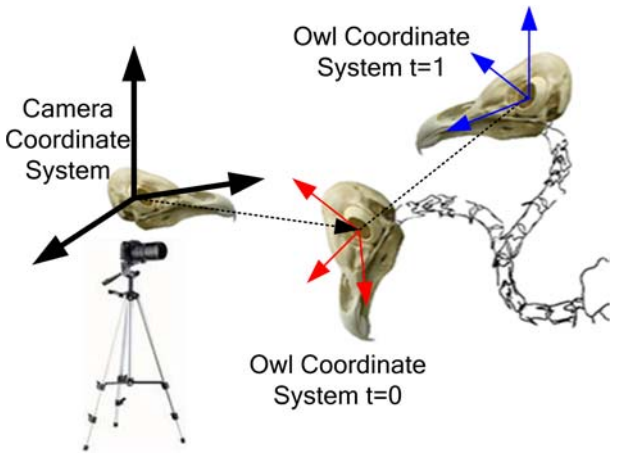

Fig. 1 Coordinate systems used in the experiments. The movements of the owl were recorded in the camera coordinate system (*left*). Analysis was done in both the camera coordinate system and the owl coordinate system (*right*). The figure shows the barn owl's skull at two states ($t = 0$, $t = 1$), indicating that head rotation might also be accompanied by translation of the center of mass

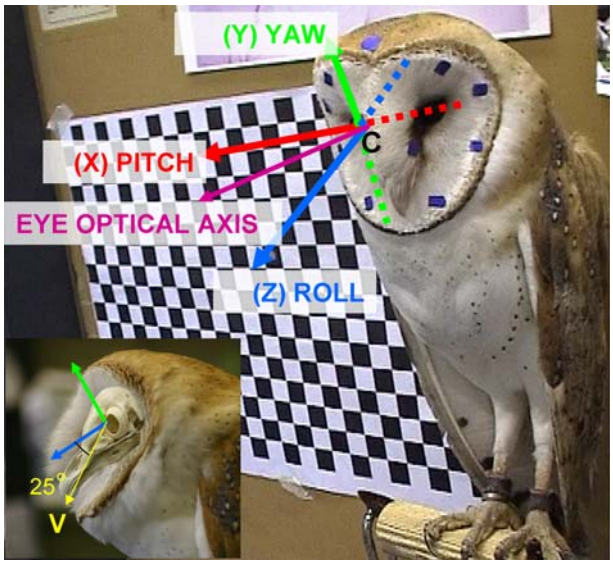

Fig. 2 Owl intrinsic coordinate system. The origin was chosen to be the mean position between the eyes. The pitch axis aligns with eye's center. The roll axis approximates the owl's actual gaze, and is approximately 25° elevated from the line joining the origin and the tip of the beak (see *inset* at *lower left*). The yaw axis is perpendicular to both the pitch and roll axis in a right-hand Cartesian coordinate system. Eye optical axis is assumed to diverge from the roll axis by 30°

1998). In this description, the movement is described as $P' - s = R_{\hat{n},\Theta}(P - s) + t\hat{n}$. $R_{\hat{n},\Theta}$ represents a rotation of Θ degrees about the rotation axis $\hat{n}$. The point s lies on $\hat{n}$ at the shortest distance to the origin. In this representation, the amount of translation (t) is minimized and occurs only along the rotation axis. This representation describes head rotations well, but is not suitable to describe head translations, because when Θ is zero, $\hat{n}$ is not uniquely defined. The two representations are equivalent mathematically, as can be seen from $T = t\hat{n} + (I - R_{\hat{n},\Theta})s$. In the following sections, we will use both representations to analyze our data.

The axes of the camera coordinate system are defined according to the optical axis of the lens and the plane of the CCD sensor. However, the intrinsic owl's coordinate system is unknown. Thus, a ''meaningful'' coordinate system must be selected and defined according to visible head features. We used the position of the two eyes and the tip of the beak to define the owl's head coordinate system. The main reasons to choose these features are that they are visible and easy to detect in the photographs of an owl's head. The origin of this coordinate system is set to be centered between the two eyes. The pitch axis aligns with the center position of the two eyes. The roll axis was determined to be what is thought to be the animal's direction of gaze. This direction is known from behavioral experiments carried out in other contexts (Endler, personal communication). In our coordinate system, we describe this direction relative to the tip of the beak. If we define the direction from the mean position between the eyes to the tip of the beak as V, then the roll axis is defined by rotating V about the pitch axis by approximately 25° upward (Fig. 2).

In our configuration the fixed reference frame aligns with the camera coordinate system. Measurements of $[R(t), T(t)]$ should be understood in the following manner: in order to bring the owl's head from the camera to its current position at time t, one needs to rotate it by amount $R(t)$, and translate it by amount $T(t)$. To obtain a more meaningful description of movement, the data can be transformed to represent movements in the owl coordinate system. For that, a specific reference frame must be chosen. The mathematical formulation for this procedure is: given $[R(t), T(t)], [R(t+k), T(t+k)]$, where t is the time of the reference frame, k is the time passed, the R–T description of the movement represented in the owl coordinate system is obtained from $[R(t), T(t)]^{-1} \times [R(t+k), T(t+k)]$. It is important to describe movements in the owl coordinate frame, rather than the camera coordinate system since they are independent of measuring device position and orientation (Fig. 3).

Head tracking system

In this study we used a novel head tracking system which was recently developed (S. Ohayon and E. Rivlin,

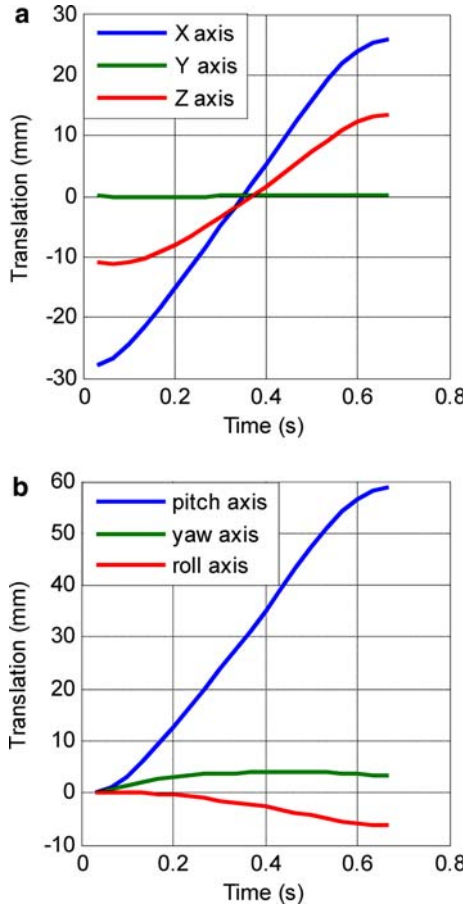

Fig. 3 Representation of a movement in the different coordinate systems. For this translational movement both *X*- and *Z*-axis movements dominate in the camera coordinate system (**a**), while the owl coordinate system demonstrate a movement mainly along the pitch axis (**b**)

in preparation). The system tracks an animal's head in 3D using a single camera, and reports the rigid-body transformations $[R(t), T(t)]$. To track the head in a precise way several markers were attached to the animal's head. These markers did not interfere with the owl's natural behavior in any way. In our configuration 12–14 markers were used. The markers were small blue paper stickers with a diameter of 5–10 mm (Fig. 4). In the following, we describe how the system was used but omit the implementation details. The interested reader can find a more detailed description which includes the mathematics and algorithms in S. Ohayon and E. Rivlin (in preparation).

The accuracy of the system was evaluated in a series of tests. A calibration object was tracked at known positions and orientations. Tracking results were compared to reference measurements of the calibration object and indicated that under ideal conditions the absolute positional accuracy has a standard deviation of 2.3 mm, while angular accuracy has a standard deviation of 0.47°.

Camera calibration

In order to extract correct useful metric information from a video sequence, several camera parameters must be evaluated (focal length, radial distortion coefficients, divergence from optical axis). These parameters can be estimated using automated calibration algorithms. The calibration algorithm we chose was easy to implement and consisted of filming a checkerboard pattern (Fig. 4). All necessary camera parameters could be estimated from several images of the checkerboard pattern (Zhang 2000).

Marker calibration

In addition to camera calibration, the relative 3D Euclidean distances between markers on the owl's head needed to be computed. An accurate description of the relative distances is required to calculate the position and orientation of the head in 3D using a single camera. The markers define a 3D model which approximates the surface of an owl's head. The model was acquired using several photos taken with the checkerboard pattern in the background (Fig. 4). In these photos, the owl was sitting on a perch at a distance of 10–20 cm in front of the checkerboard pattern. The background pattern was used as a reference frame, from which position and size measurements could be inferred. For further details please refer to S. Ohayon and E. Rivlin (in preparation). The calibration was repeated at the beginning of each experiment.

Fig. 4 Several shots from a calibration sequence. Camera internal parameters (focal length, optical axis position in the image, radial distortion) were evaluated from the checkerboard pattern in the *background*

Stimulus

A small moving platform on wheels was constructed (the *ChickMobile*) to simulate live prey movement. The platform could be controlled from several meters away using a wireless remote. A dead chick or parts of it were mounted on top of the platform (Fig. 5). The tracking phase of an experiment started with the insertion of the *ChickMobile* into the room. During this phase, the owl was filmed using the single stationary camera. The observer watched the owl's behavior and controlled the *ChickMobile* accordingly.

Experimental arrangement

The experiments took place at two locations. Owl SL was tested in the bird aviary and was able to move freely. The cage measured 165 cm in width, 425 cm in length and 250 cm in height (Fig. 5). No attempt was made to change surrounding temperature or auditory levels. The light source was a regular fluorescent bulb which produced a light level of 10 cd/m^2. The light level was kept constant during the experiments. The cage contained a perch located at 175 cm above the ground (Fig. 5). Stimulus location varied across the room. While sitting on the perch, the owl viewed the stimulus at angles of 37° ± 20°, with respect to the horizon. The observer was outside the cage and outside the bird's visual field to monitor experiments.

Fig. 5 Example of an attack sequence of owl SL in the experimental chamber. The owl was initially sitting on his favorite perch and was directing head movements towards the prey. Then the bird started to fly, correcting the orientation in mid-flight. Note the *ChickMobile* with a piece of a chick on top

Owl PT was tested mainly in a large soundproof cage, tied to a perch. This room measured 310 cm in width, 420 cm in length and 315 cm in height. The height of the perch was 180 cm. The owl viewed the prey at angles of 25° ± 5°. The light source produced a light level of about 10 cd/m^2.

Experiments were conducted in the afternoon. Each experiment was composed of two phases: calibration and tracking. First, markers were attached to the owl's head, and several photographs of the owl with a checkerboard pattern in the background were taken. These measurements were used to calibrate both camera and model. Afterwards, the owl was taken to the experimental room. A stationary camera was positioned on a tripod of variable height (120 ± 40 cm) at an angle of 45° ± 10° to the favorite perch of the animal. The camera never obstructed the owl's line of sight to stimuli. The *ChickMobile* was inserted into the room and was moved to gain the owl's attention. Once the owl fixated on the *ChickMobile*, the platform remained stationary and produced no sound.

Data collection

A digital video camera (Sony DCR-TRV33) was used for recording in interlaced mode at 30 frames per second. Image resolution was set to the maximum (720 × 576 pixels) and a de-interlaced algorithm was used to keep image aspect ratio. Camera focal length was chosen such that 1 mm was projected to 4–7 pixels. Data were transferred to the computer using fire-wire IEEE 1394 cable, and video stream was stored using video capturing software.

Long film sequences were recorded and were manually inspected to extract shorter sequences that showed the owl several seconds before he attacked the prey. All data sequences were analyzed while the *ChickMobile* was stationary. Special tracking software was developed for automatic analysis of the captured sequences. The analysis was preformed offline. The locations of the markers in the video sequences were automatically detected. This information was used to recover the 3-D position and orientation of the head.

Data filtering

The output of the software which analyzed the video sequences was an array of noisy six-dimensional vectors

which represented head position and orientation (using Euler angles) at any given frame. The noise originated from inaccuracies in detecting the exact position of markers in the image. To filter out the noise and to create smooth profiles, we used the following methods. First, a median filter with window size of 3 was applied to remove gross errors in the estimation of position or orientation that were a result of tracking failures. However, such failures occurred rarely and were brief in duration (1 frame). Then, an anisotropic diffusion filter was used. This filter has the property of smoothing the data while preserving the position of abrupt changes (Perona and Malik 1990). It was important to keep the localization of such changes in the signal since they were used for segmentation of the long sequence into the different movements the owl made. Afterward, spline functions were fitted to the profiles and were used to compute smooth velocity and acceleration profiles using analytical differentiation.

Data analysis

Angular velocity was calculated by converting the Euler representation to rotation-vector representation and measuring the change of angle between consecutive frames. The change of head angle was equivalent to the change in gaze. Translational velocity was computed by: $V = \sqrt{\dot{X}^2 + \dot{Y}^2 + \dot{Z}^2}$. The accuracy of the absolute positional and angular variation of the system was given before. The more important measure for the subsequent analysis is the accuracy of the relative position and orientation. This accuracy depends on the amount of an object's motion, leading to motion blur and inexact detection of markers. We determined an accuracy of 1 mm in relative position, equivalent to 30 mm/s in translational velocity, and 0.33° in relative orientation, equivalent to 10°/s in angular velocity for our system (see thick red lines in Fig. 6d).

When angular velocity is zero, the movement can be represented by the translational movement of the center of mass. This is equivalent to a curve in 3D. In differential geometry any curve may be represented by its curvature and torsion. These two measures are invariant under rigid body transformation, which means that if the curve goes through a global rotation and translation, the representation does not change. Curvature gives a measure of how much a trajectory is curved (units: degrees/millimeters), while torsion measures how much the trajectory can be fitted to a single plane (Pressley 2001). For instance, a circle has a constant curvature and zero torsion, a line has zero curvature and zero torsion and a helix has constant torsion and constant curvature. Significant, local maxima of curvature (values above 0.15°/mm) were used to partition the 3D curves into straight and curved segments.

To determine whether a segment was curved or straight, an ellipse was fitted to the segment and its eccentricity was calculated. Ellipse eccentricity is the ratio between the foci distance and the major axis length. Eccentricity values range between 0 and 1, where 0 represent a circle and 1 a straight line. Therefore, eccentricity can be used as quantitative criteria to determine how much a curve is straight. Straight lines were defined as ellipses with eccentricity of > 0.98, meaning that the major axis was at least five times as long as the minor axis. This two-step approach yielded better segmentation results than relying only on absolute values of curvature.

Results

Barn owls make conspicuous head movements prior to take-off from a perch. These head movements are different from the large head saccades often induced in sound-localization experiments by stimulating from peripheral positions. Pre-attack head movements from two adult barn owls were recorded in two experimental chambers. Twenty-nine video sequences were analyzed in total: 5 of owl PT and 24 of owl SL. Video sequences are available for download at http://www.cs.technion.ac.il/~shayo. All attacks of owl SL analyzed here ended successfully with the capture of the prey item on top of the platform. The mean length of a sequence was 27 ± 16 s.

Analysis and segmentation of sequences

The profiles from a typical video sequence showing the last 25 s before attacking the prey on top of the *ChickMobile* are shown in Fig. 6. Angular velocity is characterized by short bursts, while translational velocity contains longer, oscillatory-like segments (Fig. 6d). Furthermore, there are segments of no motion at all.

The qualitative observations of translational and rotational profiles indicated a classification of movements. This segmentation was determined according to simple thresholds using velocities and accelerations of both translational and rotational components. We considered these three basic types of movements: head rotations, head translations and fixations. Limb movements, such as walking toward the end of the perch, were sparse (7 ± 5% per movie) and were not considered further.

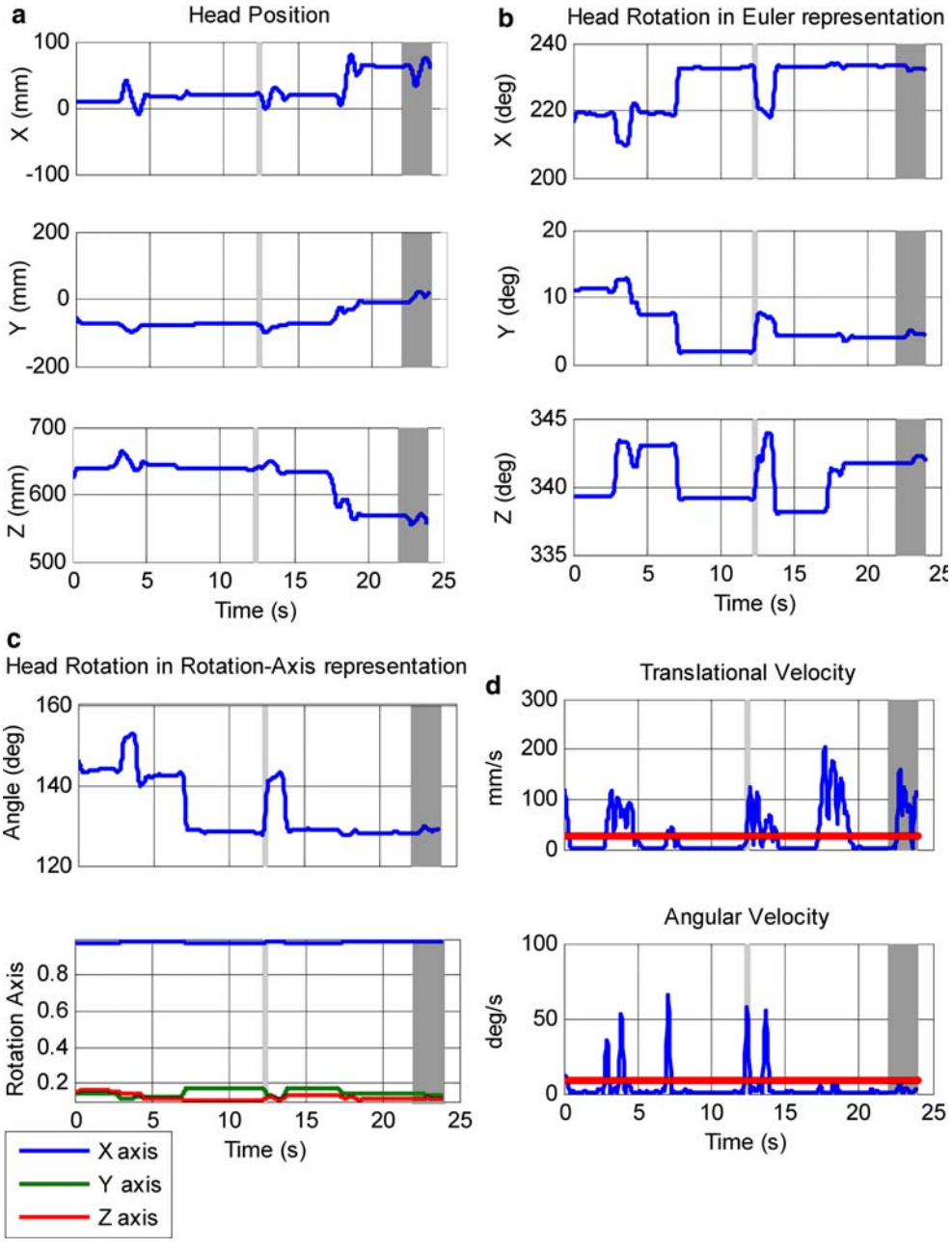

Fig. 6 Description of the barn owl's head in the camera coordinate system. **a** The position of the head, relative to the camera, is given in the center of mass representation. **b** The orientation of the head relative to the camera-coordinate system, represented in three Euler angles. **c** Head rotation angle and rotation-axis direction, relative to the camera, represented in rotation-axis description. The direction is shown by normalizing the directional components to unity. **d** Translational and angular velocities. In **a**–**d** a *light gray bar* points to a head rotation, where a *dark gray bar* indicates head translation

Head rotations were detected by searching for segments which contained angular velocity above a fixed threshold (10°/s), irrespective of translational velocity. Note that head rotations typically also contained translational component when analyzed in the center of mass representation. Fixations were determined as segments in which rotational velocity was below 10°/s and translational velocity and acceleration were lower than 30 mm/s and 450 mm/s^2, respectively. Segments with low rotational velocity (< 10°/s) and high translational velocity (above thresholds given above) were considered to be head translations.

In agreement with the qualitative observations made before, the quantitative analysis produced three distinct clusters (Fig. 7). The left lower cluster represents fixations, the right lower cluster represents head translations and the upper cluster represents head rotations. Fixations, head rotations, and head translations were similar in amount (Table 1).

Head rotations

Head rotations were short in duration (Table 1). Head rotations had both high translational and rotational

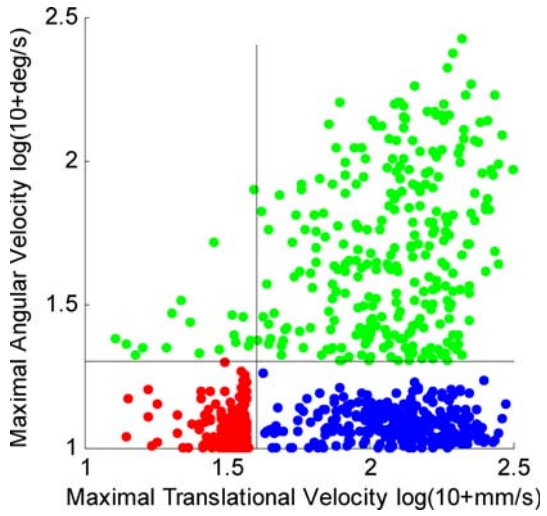

Fig. 7 Automatic classification of head movements according to their maximal velocities. Fixations (*red*) appear in the *lower left*. Peering movements (*blue*) cluster in the *lower right*. Head rotations (*green*) scatter in the *upper part* of the diagram. The *horizontal line* at 10°/s represents the threshold use to determine head rotations. The *vertical line* at 30 mm/s represents the threshold used to discriminate fixations from translations. A value of 10 was added to the velocities. This prevented negative values and gives better visualization of the categories

velocities, when plotted in the center of mass representation (Fig. 7, Table 1). Head rotations without any translation were not observed (no points in the top left most part of Fig. 7). Rotations were also analyzed using the helical representation, which allowed better understanding of the data. An example for such analysis is shown in Fig. 8. It is clear that the rotation axis direction was kept fixed (Fig. 8c), while the axis position translated mainly along the yaw axis (Fig. 8d). Even under this representation, a small translation of approximately 5 mm along the rotation axis direction is also noticeable (Fig. 8b).

One could argue that the measured translation in the center of mass representation is an artifact, caused by improper placement of the owl coordinate system's origin. In such case, the measurements of pure rotational movement will be recorded as $P' = R(t)(P + C) + T = R(t)P + [T + R(t)C] = R(t)P + T'(t)$, where C is the distance from the true rotation point and T is a constant. Thus, the recorded rotation is not affected by the misalignment, but the observed translation (T') has a direct relationship with the rotational component (R), and the distance to the true rotation point (C). If head rotations were about a fixed point or a fixed axis, we would get the same value for C during the entire head rotation. However, the analysis of 300 head rotations showed that C is not fixed and may change during the rotation by more than 10 cm. This indicates that rotation did not occur about a single point.

Generally spoken, the owl might rotate about a fixed point, a fixed axis or about a point or axis moving in 3D space. To determine which strategy the owl uses, a total of 300 head rotations were analyzed using the helical representation (Table 2). The change in gaze was relatively small (14.37 ± 13.84°). During those movements the orientation of the rotation vector remained largely constant (5.87 ± 7.22°, Table 2). These vectors were not fixed to a single position, but moved considerably, if the head size of the owl (some 4 cm) is taken as a reference (29.15 ± 23.86 mm).

To determine whether Listing's law applies to barn owl head movements, we analyzed six experiments in which the camera remained at the same position, allowing us to record all movements relative to the same position in space. Eight hundred seventy-seven head rotation-vectors were obtained and were fitted with a plane using least squares minimization. The distances between rotation vectors and this plane represent the fitting error and are measured in degrees. The standard deviation of the error was 5.9°, suggesting a poor fit. Following previous studies (Medendorp et al. 1998), we also tried to fit a second-order twisted surface. This resulted in a better fit with a standard deviation of 0.9°.

Fixation periods

Fixation, lacking any movement, was not considered as a meaningful category previously. However, during these time segments the owl was alert and looked toward the *ChickMobile*. Fixation periods occupied

Table 1 Statistics of head rotations, translations and fixations

Twenty-nine sequences	Fixation	Head rotations	Head translations
Total number of periods	272	300	284
Occurrence (per sequence)	9.38 ± 5.33	12.83 ± 10.81	9.79 ± 6.03
Duration (s)	1.15 ± 1.37	0.29 ± 0.15	0.56 ± 0.41
Percentage of time spent on movement (per sequence) (%)	48.01 ± 13.12	15.01 ± 8.11	25.84 ± 6.86
Maximal value of translational velocity (mm/s)	22.57 ± 4.17	118.38 ± 62.16	126.32 ± 54.47
Absolute value of angular velocity (°/s)	4.45 ± 3.15	49.36 ± 43.13	6.02 ± 2.81

Measurements are described as mean ± standard deviation

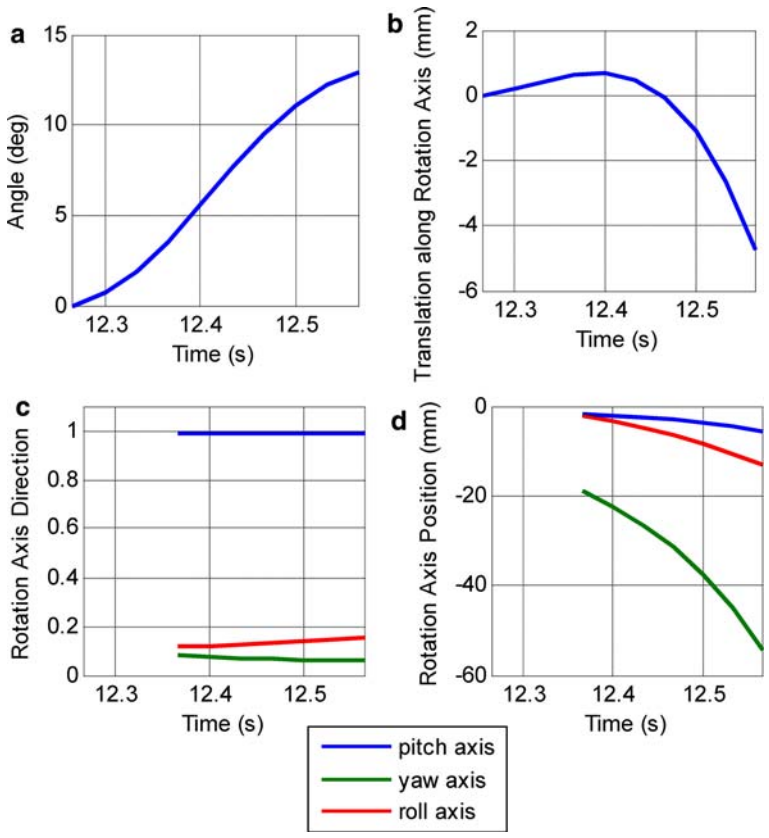

Fig. 8 Helical-axis representation of a head rotation in the owl coordinate system. **a** Rotation angle, **b** Translation along the rotation axis, **c** Shortest distance from rotation axis to the origin (position of rotation axis), **d** Rotation axis normalized to unity . Measurements in (**c**, **d**) at time 12.25–12.35 are not shown due to instability of the description to represent angles < 4°. This sequence is part of the movements marked as *light gray* in Fig. 6

Table 2 Characteristics of head rotations

Total number of head rotations	300
Change of the rotation axis orientation during head rotation (°)	5.48 ± 6.85
Change of the rotation axis position during head rotation (mm)	29.15 ± 23.86
Angular change during head rotation (°)	14.37 ± 13.84
Translation along rotation axis (mm)	9.49 ± 10.39

Measurements are described as mean ± standard deviation

almost 50% of the time when the owl became interested in the target and before it took off from the perch (Table 1). The large time percentage was mainly due to the duration (longest fixation was 6.1 s), rather to the number of occurrences (Table 1). Unfortunately, it was not possible to precisely record the position of the *ChickMobile* relative to the owl in our setup (see Outlook section in Discussion).

Head translations

Head translations were identified by their low angular velocity (6.02 ± 2.81°/s) and high translational velocity (126.32 ± 54.47 mm/s, see also lower right part of Fig. 7). Since these translations resemble peering movements as seen in other animals, we shall refer to the head translations also as peering movements. Peering rarely occurred at low light levels or toward auditory targets, suggesting a visually guided behavior. We also observed that owls would exhibit none, or very short peering movements before an attack on stationary prey items on the ground. Long and complex peering movements would occur only when the prey item had the ability to move (for example, when mounted on the *ChickMobile*).

A typical translational movement (22.5–24 s, Fig. 6 dark grey; zoomed in Fig. 9) is characterized by near zero rotational velocity and translational movement along straight lines and curved paths. The curvature measure can be used to decompose the movement into shorter motion components. For example, in the segment from 22.5–24 s (Fig. 9), two peaks of curvature were observed (Fig. 10), which indicated that this complex motion can be decomposed into three smaller components (Fig. 9e).

Similar observations were made for the other translational segments. By trial and error we found that a curvature of 0.15°/mm was a useful threshold to detect meaningful peaks. With this approach, all 284 head

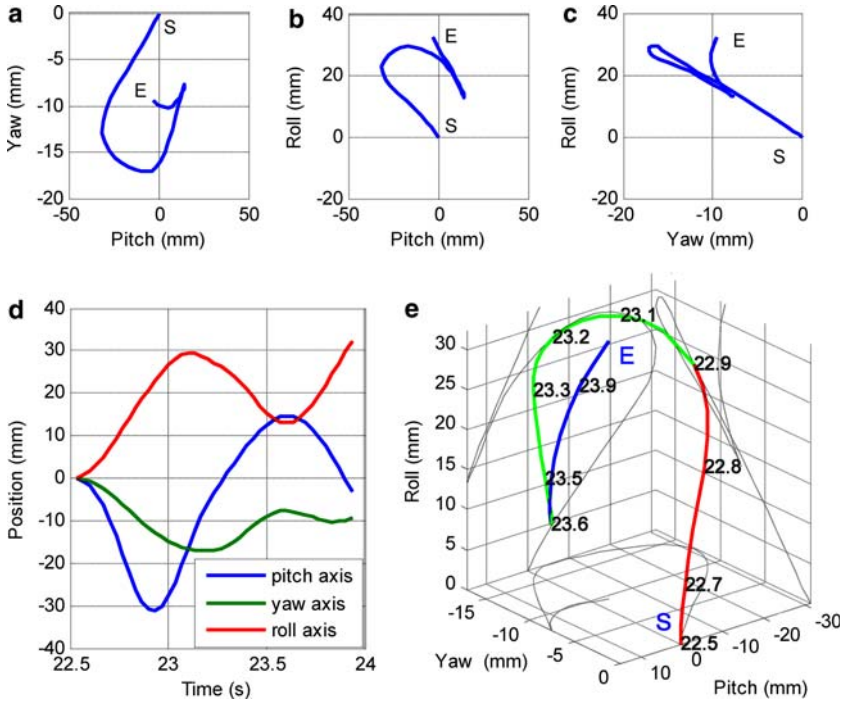

Fig. 9 Example of a head translation. **a**–**c** Orthographic projections of the movement, represented in the owl intrinsic coordinate system. "*S*" represents the starting position, "*E*" indicates the end of the movement. **d** Translational profiles. **e** Three-dimensional description of the movement. The light curves in **e** show the orthogonal projections (**a**–**c**) in the 3D frame. The *red-green-blue* colors represent the result of the automatic segmentation of the curve to its smaller components. The *numbers* along the *curve* denote the time in seconds

translations were further segmented into straight-line translations and curved translations. Using a threshold of 0.98 of eccentricity (Fig. 11) we observed 241 straight-line segments and 205 curved segments (Table 3). The eccentricity of the curved segments varied widely (Fig. 11). The length of the straight-line segments was shorter than the length of the curved segments (Table 3, Mann–Whitney *U*-test, $z = 3.44$, $P < 0.001$).

Interestingly, the directions of straight-line peering movements were not equally distributed over all angles on the unity sphere (Fig. 12). The elevation distribution was broad and could be modeled by a single normal distribution (5.42 ± 23°). The azimuth distribution had two peaks, one at –78° and the other at +83°, suggesting that the main translational direction was along the pitch axis. No bobbing behavior was observed as can be seen from the center of the plot (Fig. 12).

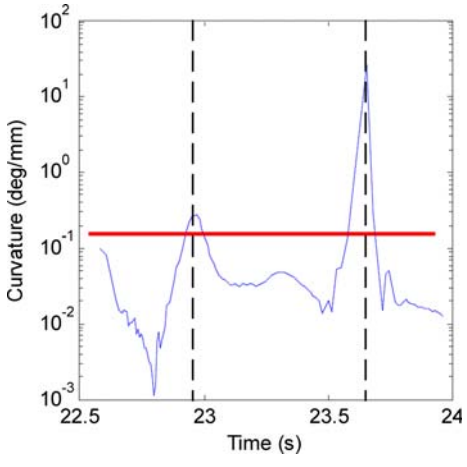

Fig. 10 Curvature. The curvature computed from the trajectory shown in Fig. 9 is plotted. *Horizontal red line* indicates the threshold used to detect significant local maxima. Two *vertical dashed lines* indicate the decomposition to three segments

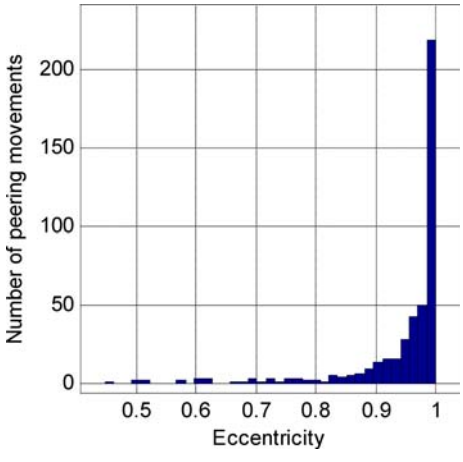

Fig. 11 Fitted ellipse eccentricity of translational segments (peering movements). Histogram of occurrences including four hundred forty-six cases. Values range between 0 (circular trajectory) and 1 (straight line)

Table 3 Characteristics of peering movements

	Straight-line segments	Curved segments
Number of segments	241	205
Length (mm)	26.69 ± 18.94	33.77 ± 22.52
Fitted ellipse eccentricity	0.99 ± 0.005	0.88 ± 0.11

Measurements are described as mean ± standard deviation

Complex movements

Until now, we have considered the basic motion components (fixations, head rotations, translations along a straight line or curved path) separately. However, these basic motions appear adjacent and can be combined to form a complex movement. For example, we could detect in our data a repeated pattern such as the one deposited in Fig. 13. A total of eight occurrences of similar movements could be found in our data. All movements started with a small (3.16 ± 2.62°) and brief (0.16 ± 0.08 s) head rotation about the roll axis, followed by two translational movements along a straight line, and ended with a fixation. The direction of the translation in the owl's coordinate system was either [70° azimuth, –20° elevation], or [–70° azimuth, –20° elevation]. The length traversed along each one of these translations was 45.72 ± 7.78 mm.

Discussion

To the best of our knowledge, the data presented here provide the most detailed quantitative investigation of pre-attack behavior in barn owls. Nevertheless, the analysis of the basic components is only a first step to understand the barn pre-attack motor behavior. A study of the functional consequences of the head movements will reveal their role in visual information processing (S. Ohayon et al., in preparation). We observed head rotations about moving (parallel) axes, two basic types of head translations (straight line, curved), and fixations. We consider these to be basic elements of motion, of which a more complex behavior can be created. In the following we discuss first our approach to measure head movements and then our findings with respect to the suggested basic motion elements. We conclude with some speculations regarding the possible functional relevance of these head movements with respect to prey capture.

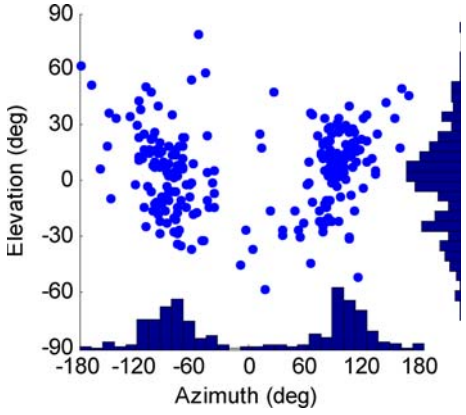

Fig. 12 Directions of straight-line peering movements. The directions of the movements (two hundred forty-one cases) are represented as azimuth and elevation in the owl coordinate system. The direction [0, 0] represents the roll axis, the direction [–90, 0] points aligns with the negative pitch axis, while the direction [90, 0] represent the positive pitch axis

Measuring head movements

Most studies, both in human and animals, have focused on the rotational components of head movements (e.g. Robinson 1963; Knudsen et al. 1979; Du Lac and Knudsen 1990). The common representation used was that of rotation vectors (Haustein 1989). However, this representation is incomplete, since it does not account for the position of the rotational vector, which can change considerably during a movement (Medendorp et al. 1998). Indeed, we observed significant translational components during head rotations in the center of mass representation. Likewise, measurements of head translational components with respect to a global reference frame may be unreliable, unless head orientation is taken into account (van der Willigen et al. 2002). Our representation, on the other hand, is complete and provide results which are comparable to commercially available wired systems.

Motion primitives

Previous studies of motor behavior in animals have reported that complex motion can be decomposed to orthogonal motion generators or a linear combination of basic motion primitives (Masino and Knudsen 1990; Bizzi et al. 1995; Mussa-Ivaldi and Bizzi 2000). In this study, several basic elements of motion were suggested as possible motion primitives, from which complex pre-attack behavior can be obtained. Since the previous study of Masino (Masino and Knudsen 1990) did not take into account the translational component of head rotations, it is unknown whether the head rotations we observed can be elicited using electric stimulation at a single site, or require a more complex activation pattern which controls translational component of the head as well.

The pure translation movements along a straight line we observed are very interesting, since they require a solution of a complex motion planning problem (generating a movement along a straight line using rotating joints). It will be valuable to discover in the future whether orthogonal translational generators also exist in the barn owl.

Head rotations

The six degrees of freedom description of head movement we obtained showed that when the head is turned to a new direction both rotational and translational components are present, indicating that the movement is not a pure rotation about a single fixed axis. Owls have a flexible neck which contains 13 vertebrae and about 30 muscles pairs (Masino and Knudsen 1990). The helical axis representation showed that the position of the rotation axis changes considerably during a head rotation, which suggests a complex interaction of neck muscles. The translational component along the rotation axis we measured was three times larger than in humans (Medendorp et al. 1998). There might be several explanations for this observation. The anatomical structure of a neck joint might not allow a pure rotation about a single point, which would result in a small translational component when the joint is moving. Multiple joints which might co-participate during a head rotation could then lead to a relative large, cumulative translational component. Yet another possibility is that toward the end of the rotational movement, a translational movement along the rotation axis started. More research is necessary to determine the exact cause.

We found the maximal velocity and amplitude during head rotations to be considerably lower than the one observed during gaze change toward sound sources (Knudsen et al. 1979; Wagner 1993) and in stimulation studies (Du Lac and Knudsen 1990; Masino and Knudsen 1990, 1993). In those studies, head saccades had maximal angular velocities that depended on saccade amplitude and were as high as 800°/s. The low velocities and amplitudes we observed are probably task related: during pre-attack behavior the owl mainly

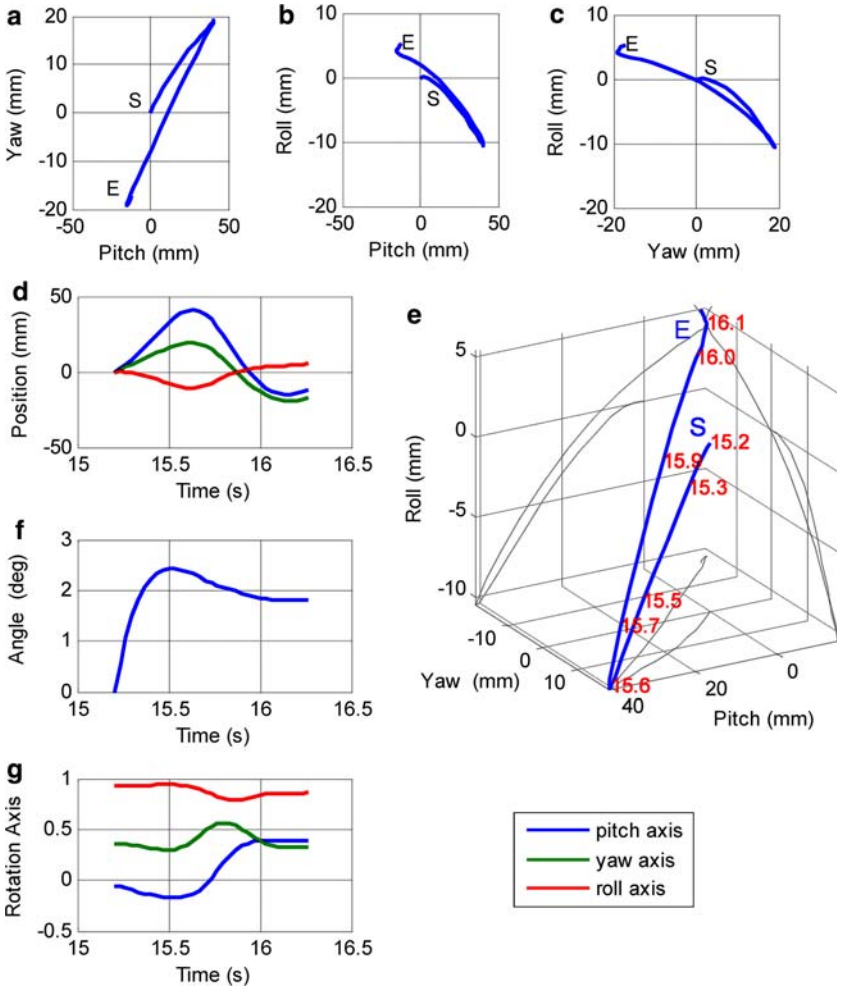

Fig. 13 An example of a complex movement. **a**–**c** Orthographic projections of the translational components. **d** Translational profiles. **e** Three-dimensonal description of the movement in the owl coordinate system. **f**, **g** Head angle and direction of rotation axis during the movement. Other symbols are as Fig. 9 legend

focused its gaze at the interesting point, the prey on the *ChickMobile*, which was already located in frontal visual space. The saccade that brought the target into this position has been analyzed elsewhere in much detail (Du Lac and Knudsen 1990; Masino and Knudsen 1990; Wagner 1993; Saberi et al. 1998) and was not of interest here. We were more interested in describing the small rotations, like a small roll movement before a translation (Fig. 13) that have not been investigated before. Such movement will cause the retinal image to rotate, thus, bringing the object of interest to a specific orientation in the retinal coordinate system.

Previous studies in owls have suggested that eye movements play only a limited role in determining gaze (Steinbach and Money 1973; Knudsen et al. 1979; Du Lac and Knudsen 1990; Masino and Knudsen 1990, 1993). Therefore, head movements can be considered as the primary mechanism in determining gaze. In our study head rotations occurred about an axis which had an almost fixed orientation. However, unlike the fixed rotation-vector position in eye movements, the position of this axis changed considerably during the rotational movement. While the observed rotation-vectors did not lie on a flat plane, suggesting a violation of Listing's law, they could be well described by a second-order surface, which is in close agreement with Donder's law. These observations are similar to the results reported by Medendorp in his study of human head rotations (Medendorp et al. 1998) and support the hypothesis that biological system uses a smaller number of parameters to control motion than the available number of degrees of freedom.

Head translations

The velocity profiles of head movements indicated segments of pure translational movement. Neither translational velocity nor amplitude was constant during these translational movements. The head was kept at a fixed orientation while it translated along complex trajectories in 3D. Some of the head translations resembled peering movements. Peering is commonly described as self-induced side-to-side movements in the horizontal plane along the pitch axis (Wallach and O'Connel 1953; Collett 1978; Kral and Poteser 1997; Kral and Devetak 1999). The resulting motion parallax can be used to determine either relative or absolute distances between the observer and objects (van der Willigen et al. 2002; Kral 2003). While most peering movements previously reported were along the pitch axis, there is evidence that such movements may have a more complex nature, such as translation along other axes and possibly involve rotations along the yaw axis (Wagner 1989; Kral and Devetak 1999). Indeed, in our experiments we have observed translations along other axes than the pitch axis. These directions were not confined to the horizontal plane. We did not find significant rotational velocity during peering in our data, but this may be due to the specific pre-attack situation or limitations in the angular resolution of our tracking system. We note that counter rotation along the yaw axis during sideways peering movements would allow to measure distance by taking into account both the amount of rotation and of translation of the head (Wagner 1989; Kral and Devetak 1999). However, recovering absolute depth is simpler when there are no rotational components. In this case, the distance between the observer and objects can be expressed as a linear relationship between instantaneous head translation velocity and optical flow. Moving the head only along the pitch axis obviously reduces the problem even further (Bruss and Horn 1983; Lewis and Nelson 1998; Katsman and Rivlin 2003).

Outlook

Our basic assumption is that pre-attack head movements are driven by functional needs which are closely related to the task at hand. Prey capture is a complex task which involves detection, identification and possible motion planning. We speculate that the observed peering-like translational movements are used to obtain distance estimation to the target. Similar behavior was reported in locusts and mantids in the context of distance estimation to landing sites or prey (Sobel 1990; Kral and Poteser 1997). The functional role of fixations and rotations is more difficult to unravel. The data obtained with two simultaneous cameras should improve our understanding of these movements. Preliminary experiments with a tiny wireless head mounted camera yielded promising results (Ohayon et al., in preparation).

We have already indicated how the basic components might be used sequentially or combined simultaneously to produce a vast repertoire of motor behaviors (Fig. 13, see also Martin 1977; Bizzi et al. 1995). For example, we could ''compose'' a type of complex movement which was repeatedly observed in several experiments. This complex movement contained head rotation, back and forth translation along the same direction, and a fixation. Such repetitive movements are a good indication of an animal's behavior (Perner 2001; Goldengerg et al. 2005). While the functional role of the movements is still unknown, we speculate that head rotation about the roll axis is used to align the retinal image to a specific orientation. The back and forth translational movement could then be used to infer information from radial flow

fields (Martin and Katzir 1999). Future research will focus on detecting more complex movements and their basic components using advanced pattern recognition techniques.

Acknowledgements We would like to thank the coordinator of the Bursary program for Israeli students, at the Center of North Rhine-Westphalia, Dr. Arne Claussen, who made Shay Ohayon's visit to Aachen possible. The experimental procedures were approved by the Regierungspräsidium Köln.

References

Bizzi E, Giszter S, Loeb E, Mussa-Ivaldi F, Salteil P (1995) Modular organization of motor behavior in the frog's spinal cord. Trends Neurosci 18:442–446

Bruss AR, Horn BKP (1983) Passive navigation. Comput Vis Graph 21:3–20

Campbell LW, Bobick A (1995) Recognition of human body motion using phase space constraints. In: International conference on computer and vision, Cambridge, pp 624–630

Collett TS (1978) Peering—a locust behaviour pattern for obtaining motion parallax information. J Exp Biol 76:237–241

Crawford JD, Martinez-Trujillo JC, Klier EM (2003) Neural control of three-dimensional eye and head movements. Curr Opin Neurobiol 13:655–662

Du Lac S, Knudsen EI (1990) Neural maps of head movement vector and speed in the optic tectum of the barn owl. J Neurophysiol 63:131–146

Glenn B, Vilis T (1992) Violations of Listing's law after large eye and head gaze shifts. J Neurophysiol 68:309–318

Goldengerg R, Kimmel R, Rivlin E, Rudzsky M (2005) Behavior classification by eigen decomposition of periodic motions. Pattern Recognit 38:1033–1043

Haker H, Misslisch H, Ott M, Frens MA, Henn V, Hess K, Sandor PS (2003) Three-dimensional vestibular eye and head reflexes of the chameleon: characteristics of gain and phase and effects of eye position on orientation of ocular rotation axes during stimulation in yaw direction. J Comp Physiol A 189:509–517

Haustein W (1989) Considerations on Listing's law and the primary position by means of a matrix description of eye position control. Biol Cybern 60:411–420

Howard IP (2002) Seeing in depth. Basic mechanisms, vol 1. I Porteous Publishing, Ontario

Katsman I, Rivlin E (2003) The mantis head camera (why the praying mantis is so good at catching its prey). In: IEEE international conference on image processing, pp 612–617

Knudsen EI, Blasdel GG, Konishi M (1979) Sound localization by the barn owl *(Tyto alba)* measured with the search coil technique. J Comp Physiol 133:1–11

Konczak Jr (2005) On the notion of motor primitives in humans and robots. In: Proceedings of the 5th international workshop on epigenetic robot, Nara, vol 123. Lund University Cognitive Studies, pp 47–54

Kral K (2003) Behavioural–analytical studies of the role of head movements in depth perception in insects, birds and mammals. Behav Processes 64:1–12

Kral K, Devetak D (1999) The visual orientation strategies of *Mantis religiosa* and *empusafasiata* reflect differences in the structure of their visual surroundings. J Insect Behav 12:737–752

Kral K, Poteser M (1997) Motion parallax as a source of distance information in locusts and mantids. J Insect Behav 10:145–163

Lewis MA, Nelson ME (1998) Look before you leap: peering behavior for depth perception. In: Proc 5 Simul Adapt Behav, pp 98–103

Martin GR (1977) Absolute visual threshold and scotopic spectral sensitivity in the tawny owl (*Strix aluco)*. Nature 268:636–638

Martin GR, Katzir G (1999) Visual fields in short-toed eagles (*Circaetus gallicus* (*Accipitridae)*) and the function of binocularity in birds. Brain Behav Evol 53:55–66

Masino T, Knudsen EI (1990) Horizontal and vertical components of head movement are controlled by distinct neural circuits in the barn owl. Nature 345:434–437

Masino T, Knudsen EI (1993) Orienting head movements resulting from electrical microstimulation of the brainstem tegmentum in the barn owl. J Neurosci 13:351–370

Medendorp WP, Melis BJM, Gielen CCAM, van Gisbergen JAM (1998) Off-centric rotation axes in natural head movements: implications for vestibular reafference and kinematic redundancy. J Neurophysiol 79:2025–2039

Moeslund TB, Reng L, Granum E (2005) Finding motion primitives in human body gestures. Gesture Workshop 2005, Berder Island, pp 31–33

Mussa-Ivaldi F, Bizzi E (2000) Motor learning through the combination of primitives. Philos Trans R Soc Lond B Biol Sci 355:1755–1769

Perner P (2001) Motion tracking of animals for behavior analysis. Lect Notes Comput Sci 2059:779–786

Perona P, Malik J (1990) Scale-space and edge detection using anisotropic diffusion. IEEE Trans Pattern Anal Mach Intell 12:629–639

Pressley A (2001) Elementary differential geometry. Springer Undergraduate Mathematics Series. ISBN: 1-85233-152-6

Robinson D (1963) A method of measuring eye movement using a scleral search coil in a magnetic field. IEEE Trans Biomed Eng 10:137–145

Saberi K, Farahbod H, Konishi M (1998) How do owls localize interaurally phase-ambiguous signals? Proc Natl Acad Sci USA 95:6465–6468

Sobel EC (1990) The locust's use of motion parallax to measure distance. J Comp Physiol A 167:579–588

Steinbach MJ, Money KE (1973) Eye movements of the owl. Vision Res 13:889–891

Troje NF, Frost BJ (2000) Head-bobbing in pigeons: how stable is the hold phase. J Exp Bio 203:935–940

Tweed D, Cadera W, Vilis T (1990) Computing three-dimensional eye position quaternions and eye velocity from search coil signals. Vision Res 30:97–110

Wagner H (1982) Flow-field variables trigger landing in flies. Nature 297:147–148

Wagner H (1989) Peering in barn owls. In: Erber J, Menzel R, Pflüger HJ, Todt DG (eds) Neural mechanisms of behavior. Thieme Verlag, New York, pp 238–239

Wagner H (1993) Sound-localization deficits induced by lesions in the barn owl's space map. J Neurosci 13:371–386

Wallach H, O'Connel DN (1953) The kinetic depth effect. J Exp Psychol 45:205–217

van der Willigen RF, Frost BJ, Wagner H (2002) Depth generalization from stereo to motion parallax in the owl. J Comp Physiol A 187:997–1007

Zeil J (1993) Orientation flights of solitary wasps (*Cerceris; Sphecidae; Hymenoptera*): I. description of flight. J Comp Physiol A 172:189–205

Zhang Z (2000) A flexible new technique for camera calibration. IEEE Trans Pattern Anal Mach Intell 22:1330–1334